Electronic Supplementary Material (ESI) for Soft Matter.

Electronic Supplementary Information (ESI)

Active shape oscillations of giant vesicles with cyclic closure and opening of membrane necks

Simon Christ[a], Thomas Litschel[b], Petra Schwille[b], and Reinhard Lipowsky*[a]

[a] *Theory and Bio-Systems, Max Planck Institute of Colloids and Interfaces, Science Park Golm, 14424 Potsdam, Germany*

[b] *Cellular and Molecular Biophysics, Max Planck Institute of Biochemistry, 82152 Martinsried, Germany*

This Electronic Supplementary Information contains the supplementary sections S1, S2, and S3, the supplementary Figs. S1, S2, and S3 as well as the captions of Movie1 and Movie2.

In Section S1, we review the shape equations as originally derived in Ref. [1] and previously applied to the engulfment of nanoparticles in Ref. [2]. In addition, we describe the scheme that we used to regularize these shape equations close to the south and north pole of the vesicle, where the radial coordinate r vanishes. The shape is parametrized by the arc length s of the shape contour. The south pole is located at $s = 0$, the north pole at $s = s_1$ which defines the total arc length s_1. The regularization scheme is based on Taylor expansions for small arc length s around the south pole and for small deviations $\epsilon = s_1 - s$ around the north pole.

In Section S2, we introduce rescaled and dimensionless variables which involve two different length scales. The arc length s is rescaled by the total arc length s_1 which leads to the dimensionless arc length $\bar{s} \equiv s/s_1$ while all other quantities that have the dimension of a length or a curvature are rescaled using the the vesicle size R_{ve} as introduced in eqn (3) of the main text. We then express both the shape equations and the regularization scheme in terms of these rescaled variables, which now involve the dimensionless ratio $\mho \equiv s_1/R_{\mathrm{ve}}$ as an additional parameter. Finally, in Section S3, we describe the protocol for the numerical solution of the rescaled shape equations. This protocol combines the Taylor expansions at the two poles with the solution for intermediate values of the arc length. The details of our computational procedure, as described in Sections S2 and S3, have not been published before but should be useful for future studies.

S1 Shape equations for axisymmetric shapes

Contour parametrization and principal curvatures. We consider an axisymmetric vesicle shape and denote the Cartesian coordinate along the rotational symmetry axis by z. The shape of such a vesicle is completely determined by its 1-dimensional shape contour as displayed in Fig. S1. We parametrize the contour line by its arc length s and choose the contour point with $s = 0$ to be the south pole of the vesicle. The shape

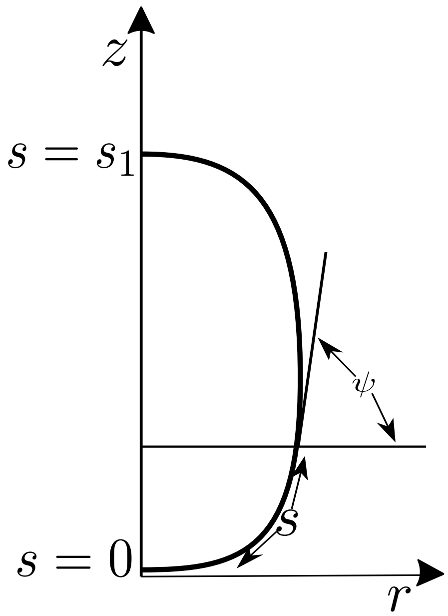

Figure S1: Contour line of an axisymmetric shape that is rotationally symmetric with respect to the z-axis. The shape of this line is parametrized in terms of the arc length s, the tilt angle $\psi = \psi(s)$, and the radial coordinate $r = r(s)$. The arc length s measures the distance along the contour line from the south pole with $s = 0$ and attains its maximum value $s = s_1$ at the north pole. The tilt angle ψ describes the angle between the radial coordinate r and the tangent to the contour. The two shape parameters $r(s)$ and $\psi(s)$ are related via $\mathrm{d}r/\mathrm{d}s = \cos(\psi)$, a constraint that is imposed by the Lagrange multiplier function $\gamma(s)$.

of the contour is then described by the tilt angle $\psi = \psi(s)$ and the radial coordinate $r = r(s)$, both of which vary with s. [1] The two principal curvatures, C_1 and C_2, are given by

$$C_1 = \frac{\mathrm{d}\psi}{\mathrm{d}s} \equiv \dot{\psi} \quad \text{and} \quad C_2 = \frac{\sin\psi}{r} \tag{S1}$$

which implies the mean curvature

$$M = \frac{1}{2}(C_1 + C_2) = \frac{1}{2}\left(\dot{\psi} + \frac{\sin\psi}{r}\right) . \tag{S2}$$

Here and below, a dot indicates the derivative with respect to the dimensionful arc length s.

Bending energy and shape energy. Using this contour parametrization, we now rewrite the bending energy E_{be} as given by eqn (1) in the main text which leads to

$$E_{\mathrm{be}} = 2\pi\kappa \int_0^{s_1} \mathrm{d}s \, \frac{r}{2}\left(\dot{\psi} + \frac{\sin\psi}{r} - 2m\right)^2 . \tag{S3}$$

where s_1 denotes the total arc length of the contour line. The shape energy F in eqn (2) of the main text now becomes [1]

$$F = 2\pi\kappa \int_0^{s_1} \mathrm{d}s \, L(\psi, \dot{\psi}, r, \dot{r}, \gamma) \tag{S4}$$

where we defined the 'Lagrange function'

$$L(\psi, \dot{\psi}, r, \dot{r}, \gamma) = L_{\mathrm{be}}(\psi, \dot{\psi}, r) - \frac{\Delta P}{2\kappa} r^2 \sin\psi + \frac{\Sigma}{\kappa} r + \gamma(\dot{r} - \cos\psi) \tag{S5}$$

with the bending energy density

$$L_{\mathrm{be}}(\psi, \dot{\psi}, r) \equiv \frac{r}{2}\left(\dot{\psi} + \frac{\sin\psi}{r} - 2m\right)^2 . \tag{S6}$$

To take into account that the radial coordinate r and the tilt angle ψ are not independent but related via $\dot{r} = \cos\psi$, the Lagrange multiplier function γ has been added to the shape energy F via the contribution

$$\Delta\mathcal{F} = 2\pi\kappa \int_0^{s_1} \mathrm{d}s\, \gamma(\dot{r} - \cos\psi) \tag{S7}$$

which implies that γ has the dimension of an inverse length or curvature.

Euler-Lagrange equations of shape energy. The shape equations are now obtained as the Euler-Lagrange equations of the shape energy in eqn (S4). Using the definition $C_1 = \dot{\psi}(s) \equiv u(s)$ for the contour curvature, one obtains the shape equations in the form [1]

$$\dot{r} = \cos\psi\,, \tag{S8}$$

$$\dot{\psi} = u\,, \tag{S9}$$

$$\dot{u} = \frac{\sin\psi\cos\psi}{r^2} - \frac{\cos\psi}{r}u - \frac{\Delta P}{2\kappa}r\cos\psi + \frac{\sin\psi}{r}\gamma\,, \tag{S10}$$

and

$$\dot{\gamma} = \frac{1}{2}(u - 2m)^2 - \frac{\sin^2\psi}{2r^2} - \frac{\Delta P}{\kappa}r\sin\psi + \frac{\Sigma}{\kappa}\,, \tag{S11}$$

which represent four ordinary differential equations of first order. Note that these shape equations depend on the spontaneous curvature m as well as on the parameter combinations $\Delta P/\kappa$ and Σ/κ. Physically meaningful vesicle shapes correspond to smooth solutions of these differential equations which fulfill certain boundary conditions at the south pole with $s = 0$ and at the north pole with $s = s_1$.

Boundary conditions at south and north pole. The parametrization of the contour line as displayed in Fig. S1 implies the obvious boundary conditions

$$r(s = 0) = 0 \quad \text{and} \quad r(s = s_1) = 0 \tag{S12}$$

for the radial coordinate $r(s)$ as well as

$$\psi(s = 0) = 0 \quad \text{and} \quad \psi(s = s_1) = \pi \tag{S13}$$

for the tilt angle $\psi(s)$. The boundary values of the contour curvature $C_1 = \dot{\psi} = u$ at the two poles are denoted by

$$u(s = 0) = U_0 \quad \text{and} \quad u(s = s_1) = U_1\,. \tag{S14}$$

Finally, using the fact that the 'Hamilton function'

$$H \equiv \dot{\psi}\frac{\partial L}{\partial \dot{\psi}} + \dot{r}\frac{\partial L}{\partial \dot{r}} - L \tag{S15}$$

is conserved along the contour, we obtain the additional boundary conditions [1]

$$\gamma(s=0) = 0 \quad \text{and} \quad \gamma(s=s_1) = 0 \tag{S16}$$

for the Lagrange multiplier function $\gamma(s)$.

Partial membrane area and vesicle volume. We now introduce the partial membrane area $\Delta A(s)$ via

$$\Delta A(s) \equiv 2\pi \int_0^s \mathrm{d}s'\, r(s') \tag{S17}$$

and the partial vesicle volume

$$\Delta V(s) \equiv \pi \int_0^s \mathrm{d}s'\, r^2(s')\, \sin\psi(s')\,. \tag{S18}$$

The partial area satisfies the evolution equation and boundary conditions as given by

$$\frac{\mathrm{d}\Delta A(s)}{\mathrm{d}s} = 2\pi r \quad \text{with} \quad \Delta A(0) = 0 \quad \text{and} \quad \Delta A(s_1) = A \tag{S19}$$

with the total membrane area A as introduced in the main text. Likewise, the partial volume satisfies

$$\frac{\mathrm{d}\Delta V(s)}{\mathrm{d}s} = \pi r^2 \sin\psi \quad \text{with} \quad \Delta V(0) = 0 \quad \text{and} \quad \Delta V(s_1) = V \tag{S20}$$

with the total vesicle volume V as in the main text.

Regularization of shape equations close to the poles. The shape eqns S10 and S11 for $\dot{u}$ and $\dot{\gamma}$ contain several terms proportional to $1/r$ and $1/r^2$. In particular, each of the first two terms on the right hand side of eqn S10 diverges individually close to the poles with $r = 0$. Even though these two singularities cancel, they do impede the numerical integration of the shape equations in the vicinity of the poles. To facilitate this integration, it is convenient to regularize the equations by using Taylor expansions for the parameter functions $r(s)$, $\psi(s)$, and $\gamma(s)$ around the two poles. [1, 2]

Regularization close to south pole. The expansion around the south pole with $s = 0$ corresponds to an expansion in powers of s and has the general form

$$r(s) = \sum_{k=1} \frac{r_k}{k!} s^k \quad \text{and} \quad \psi(s) = \sum_{k=1} \frac{\psi_k}{k!} s^k \tag{S21}$$

as well as

$$u(s) = \dot{\psi}(s) = \sum_{k=1} \frac{\psi_k}{(k-1)!} s^{k-1} \qquad \text{and} \quad \gamma(s) = \sum_{k=1} \frac{\gamma_k}{k!} s^k\,. \tag{S22}$$

The boundary condition in eqn (S14) then implies that

$$u(s=0) = U_0 = \psi_1\,. \tag{S23}$$

When we insert these expansions into the shape eqns S8 - S11 and equate the polynomial coefficients, the boundary conditions at the south pole imply that all coefficients of the Taylor series can depend on the contour curvature U_0 at this pole as well as on the three parameters m, $\Delta P/\kappa$, and Σ/κ. By matching the coefficients of the expansions on both sides of the shape equations, we find the Taylor coefficients

$$r_1 = 1\,, \quad r_2 = r_4 = 0, \quad \text{and } \; r_3 = -U_0^2 \tag{S24}$$

for the radial coordinate $r(s)$ as well as the coefficients

$$\psi_1 = U_0\,, \quad \psi_2 = \psi_4 = 0\,, \tag{S25}$$

and

$$\psi_3 = \frac{3}{8}\left[-\frac{\Delta P}{\kappa} + 2U_0\gamma_1\right] = \frac{3}{8}\left[4mU_0(m-U_0) - \frac{\Delta P}{\kappa} + 2U_0\frac{\Sigma}{\kappa}\right] \tag{S26}$$

for the tilt angle $\psi(s)$. The Taylor coefficients for the Lagrange multiplier function γ have the form

$$\gamma_1 = -2U_0 m + 2m^2 + \frac{\Sigma}{\kappa} = 2m(m-U_0) + \frac{\Sigma}{\kappa}\,, \quad \gamma_2 = 0 \tag{S27}$$

and

$$\gamma_3 = \frac{2}{3}(U_0 - 3m)\psi_3 - 2\frac{\Delta P}{\kappa}U_0 \tag{S28}$$

or

$$\gamma_3 = mU_0(m-U_0)(U_0-3m) - \frac{1}{4}(9U_0 - 3m)\frac{\Delta P}{\kappa} + \frac{1}{2}U_0(U_0-3m)\frac{\Sigma}{\kappa}\,. \tag{S29}$$

Likewise, the expansion of the partial area $\Delta A(s)$ and the partial volume $\Delta V(s)$ for small s leads to

$$\Delta A(s) \approx \pi s^2 - \frac{\pi}{12}U_0^2 s^4 \quad \text{and} \quad \Delta V(s) \approx \frac{\pi}{4}U_0 s^4 \tag{S30}$$

up to order s^4.

Regularization close to north pole. The expansion around the north pole with $s = s_1$ can be performed in an analogous manner using the expansion parameter

$$\epsilon \equiv s_1 - s \quad \text{with} \quad 0 \le \epsilon \ll s_1\,, \tag{S31}$$

which represents the arc length measured from the north pole. It will be convenient to define the functions

$$r^{\rm no}(\epsilon) \equiv r(s)\,, \quad \psi^{\rm no}(\epsilon) \equiv \pi - \psi(s) \quad \text{and} \quad \gamma^{\rm no}(\epsilon) \equiv \gamma(s) \quad \text{with} \quad s = s_1 - \epsilon \tag{S32}$$

as well as the contour curvature

$$u^{\rm no}(\epsilon) \equiv \frac{{\rm d}\psi^{\rm no}(\epsilon)}{{\rm d}\epsilon} = \frac{{\rm d}\psi(s)}{{\rm d}s} = u(s) \quad \text{with} \quad s = s_1 - \epsilon\,. \tag{S33}$$

The expansion around the north pole then has the form

$$r^{\rm no}(\epsilon) = \sum_{k=1} \frac{r_k^{\rm no}}{k!}\epsilon^k \quad \text{and} \quad \psi^{\rm no}(\epsilon) = \sum_{k=1} \frac{\psi_k^{\rm no}}{k!}\epsilon^k \tag{S34}$$

as well as

$$u^{\rm no}(\epsilon) = \frac{{\rm d}\psi^{\rm no}}{{\rm d}\epsilon} = \sum_{k=1} \frac{\psi_k^{\rm no}}{(k-1)!}\epsilon^{k-1} \qquad \text{and} \quad \gamma^{\rm no}(s) = \sum_{k=1} \frac{\gamma_k^{\rm no}}{k!}\epsilon^k\,. \tag{S35}$$

The boundary condition in eqn (S14) now implies that

$$u(s = s_1) = U_1 = u^{\rm no}(\epsilon = 0) = \psi_1^{\rm no}\,. \tag{S36}$$

By again equating coefficients on the two sides of the shape equations, we now find

$$r_1^{\rm no} = 1\,, \quad r_2^{\rm no} = r_4^{\rm no} = 0\,, \quad \text{and } r_3^{\rm no} = -U_1^2\,, \tag{S37}$$

for the radial coordinate $r^{\rm no}(\epsilon)$ and the coefficients

$$\psi_1^{\rm no} = U_1\,, \quad \psi_2^{\rm no} = \psi_4^{\rm no} = 0\,, \tag{S38}$$

and

$$\psi_3^{\rm no} = -\frac{3}{8}\left[\frac{\Delta P}{\kappa} + 2U_1\gamma_1^{\rm no}\right] = \frac{3}{8}\left[4mU_1(m - U_1) - \frac{\Delta P}{\kappa} + 2U_1\frac{\Sigma}{\kappa}\right] \tag{S39}$$

for the tilt angle $\psi^{\rm no}(\epsilon)$. The coefficients for the Lagrange multiplier function $\gamma^{\rm no}(\epsilon)$ are now given by

$$\gamma_1^{\rm no} = 2m(U_1 - m) - \frac{\Sigma}{\kappa}\,, \quad \gamma_2^{\rm no} = \gamma_4^{\rm no} = 0\,, \tag{S40}$$

and

$$\gamma_3^{\rm no} = \frac{2}{3}(3m - U_1)\psi_3^{\rm no} + 2\frac{\Delta P}{\kappa}U_1 \tag{S41}$$

or

$$\gamma_3^{\rm no} = mU_1(m - U_1)(3m - U_1) + \frac{1}{4}(9U_1 - 3m)\frac{\Delta P}{\kappa} + \frac{1}{2}U_1(3m - U_1)\frac{\Sigma}{\kappa}\,. \tag{S42}$$

Likewise, we define the partial area and volume functions close to the north pole according to

$$\Delta A^{\rm no}(\epsilon) \equiv \Delta A(s_1 - \epsilon) \quad \text{and} \quad \Delta V^{\rm no}(\epsilon) \equiv \Delta V(s_1 - \epsilon)\,. \tag{S43}$$

These partial functions behave as

$$\Delta A^{\rm no}(\epsilon) \approx A - \pi\epsilon^2 + \frac{\pi}{12}U_1^2\epsilon^4 \quad \text{and} \quad \Delta V^{\rm no}(\epsilon) \approx V - \frac{\pi}{4}U_1\epsilon^4 \tag{S44}$$

for small $\epsilon = s_1 - s$ up to up to $\mathcal{O}(\epsilon^4)$ with the total membrane area A and the total vesicle volume V as in the main text.

S2 Rescaled parameters and shape equations

Rescaled parameters. Because the total arc length $s = s_1$ is an unknown, shape-dependent parameter, it is convenient to introduce the rescaled arc length

$$\bar{s} \equiv \frac{s}{s_1} \quad \text{which implies} \quad \bar{s}_1 = 1\,. \tag{S45}$$

The other quantities that have the dimension of a length or curvature are rescaled by the vesicle size $R_{\text{ve}} = \sqrt{A/(4\pi)}$ as defined in eqn (3) of the main text, which leads to the rescaled variables

$$\bar{r}(\bar{s}) \equiv \frac{r(s)}{R_{\text{ve}}}\,, \quad \bar{u}(\bar{s}) \equiv R_{\text{ve}} u(s)\,, \quad \text{and} \quad \bar{\gamma}(\bar{s}) \equiv R_{\text{ve}}\gamma(s) \quad \text{with} \quad s = s_1 \bar{s}\,. \tag{S46}$$

For the tilt angle which is dimensionless, we use the analogous notation

$$\bar{\psi}(\bar{s}) \equiv \psi(s) \quad \text{with} \quad s = s_1 \bar{s}\,. \tag{S47}$$

The resulting shape equations for these rescaled variables then depend on another dimensionless parameter, the length scale ratio

$$\mho \equiv \frac{s_1}{R_{\text{ve}}} \quad \text{with} \quad \mho \geq \pi \tag{S48}$$

where the lowest possible value $\mho = \pi$ corresponds to a spherical vesicle shape.

Rescaled shape equations. Indeed, in terms of the rescaled variables, the first three shape eqns (S8) - (S10) become

$$\frac{\mathrm{d}\bar{r}}{\mathrm{d}\bar{s}} = \mho \cos\bar{\psi}\,, \tag{S49}$$

$$\frac{\mathrm{d}\bar{\psi}}{\mathrm{d}\bar{s}} = \mho \bar{u}\,, \tag{S50}$$

and

$$\frac{\mathrm{d}\bar{u}}{\mathrm{d}\bar{s}} = \mho \left(\frac{\sin\bar{\psi}\cos\bar{\psi}}{\bar{r}^2} - \frac{\cos\bar{\psi}}{\bar{r}}\bar{u} - \frac{1}{2}\Delta\bar{P}\,\bar{r}\cos\bar{\psi} + \frac{\sin\bar{\psi}}{\bar{r}}\bar{\gamma} \right) \tag{S51}$$

with the rescaled pressure difference

$$\Delta\bar{P} \equiv \Delta P \,\frac{R_{\text{ve}}^3}{\kappa}\,. \tag{S52}$$

Likewise, the fourth shape eqn (S11) becomes

$$\frac{\mathrm{d}\bar{\gamma}}{\mathrm{d}\bar{s}} = \mho \left[\frac{1}{2}(\bar{u} - 2\bar{m})^2 - \frac{\sin^2\bar{\psi}}{2\bar{r}^2} - \Delta\bar{P}\,\bar{r}\sin\bar{\psi} + \bar{\Sigma} \right] \tag{S53}$$

with the rescaled membrane tension

$$\bar{\Sigma} \equiv \Sigma \,\frac{R_{\text{ve}}^2}{\kappa}\,. \tag{S54}$$

Rescaled partial area and volume. The rescaled partial area $\Delta\bar{A}$ of the membrane is defined by

$$\Delta\bar{A}(\bar{s}) \equiv \frac{\Delta A(s)}{4\pi R_{\mathrm{ve}}^2} = \frac{\mho}{2}\int_0^{\bar{s}} \mathrm{d}\bar{s}'\,\bar{r}(\bar{s}') \tag{S55}$$

which implies the evolution equation

$$\frac{\mathrm{d}\Delta\bar{A}(\bar{s})}{\mathrm{d}\bar{s}} = \frac{\mho}{2}\,\bar{r}\,. \tag{S56}$$

On the other hand, the rescaled partial volume $\Delta\bar{V}$ is taken to be

$$\Delta\bar{V}(\bar{s}) \equiv \frac{\Delta V(s)}{\frac{4\pi}{3}R_{\mathrm{ve}}^3} = \frac{3\mho}{4}\int_0^{\bar{s}} \mathrm{d}\bar{s}'\,\bar{r}^2(\bar{s}')\,\sin\bar{\psi}(\bar{s}') \tag{S57}$$

and satisfies the evolution equation

$$\frac{\mathrm{d}\Delta\bar{V}(\bar{s})}{\mathrm{d}\bar{s}} = \frac{3\mho}{4}\,\bar{r}^2\sin\bar{\psi}\,. \tag{S58}$$

Boundary conditions for rescaled variables. The boundary conditions for the rescaled shape functions are

$$\bar{r}(\bar{s}=0) = 0 \quad \text{and} \quad \bar{r}(\bar{s}=1) = 0\,, \tag{S59}$$

$$\bar{\psi}(\bar{s}=0) = 0 \quad \text{and} \quad \bar{\psi}(\bar{s}=1) = \pi\,, \tag{S60}$$

$$\bar{u}(\bar{s}=0) = \bar{U}_0 \quad \text{and} \quad \bar{u}(s=s_1) = \bar{U}_1 \tag{S61}$$

with the rescaled contour curvatures

$$\bar{U}_0 \equiv U_0 R_{\mathrm{ve}} \quad \text{and} \quad \bar{U}_1 \equiv U_1 R_{\mathrm{ve}} \tag{S62}$$

at the two poles as well as

$$\bar{\gamma}(\bar{s}=0) = 0 \quad \text{and} \quad \bar{\gamma}(\bar{s}=1) = 0\,. \tag{S63}$$

In addition, the boundary values for the rescaled membane area are

$$\Delta\bar{A}(\bar{s}=0) = 0 \quad \text{and} \quad \Delta\bar{A}(\bar{s}=1) = 1\,, \tag{S64}$$

those for the rescaled vesicle volume are

$$\Delta\bar{V}(\bar{s}=0) = 0 \quad \text{and} \quad \Delta\bar{V}(\bar{s}=1) = v \tag{S65}$$

with the dimensionless volume-to-area ratio v as defined in eqn (4) of the main text.

Dimensionless parameters. The shape equations and boundary conditions for the rescaled variables as described in the previous paragraphs depend on seven dimensionless parameters: the shape parameters v and $\bar{m}$, the contour curvatures $\bar{U}_0$ and $\bar{U}_1$ at the two poles, the pressure $\Delta\bar{P} = \Delta P R_{\mathrm{ve}}^3/\kappa$, the tension $\bar{\Sigma} = \Sigma R_{\mathrm{ve}}^2/\kappa$, and the length scale ratio $\mho = s_1/R_{\mathrm{ve}}$. When we consider certain fixed values of the shape parameters v and $\bar{m}$, see main text, the different branches of solutions then correspond to different values of the five parameters $\bar{U}_0$, $\bar{U}_1$, $\Delta\bar{P}$, $\bar{\Sigma}$, and $\mho$. In order to construct such solutions in practise, we need to deal with the numerical difficulties close to to two poles and to regularize the rescaled equations as well.

Regularization of rescaled equations close to south pole. Close to the south pole, the expansion of the rescaled radial coordinate $\bar{r}$ in powers of $\bar{s}$ leads to

$$\bar{r} = \bar{r}_1 \bar{s} + \frac{1}{6} \bar{r}_3 \, \bar{s}^3 + \mathcal{O}(\bar{s}^5) \tag{S66}$$

with the Taylor coefficients

$$\bar{r}_1 = \mho r_1 = \mho \quad \text{and} \quad \bar{r}_3 = \mho^3 r_3 = -\mho^3 U_0^2 \, . \tag{S67}$$

Likewise, the tilt angle ψ becomes

$$\bar{\psi}(\bar{s}) = \bar{\psi}_1 \bar{s} + \frac{1}{6} \bar{\psi}_3 \, \bar{s}^3 + \mathcal{O}(\bar{s}^5) \tag{S68}$$

with the coefficients

$$\bar{\psi}_1 = \psi_1 s_1 = U_0 s_1 = \mho \bar{U}_0 \quad \text{and} \quad \bar{\psi}_3 = \psi_3 s_1^3 \tag{S69}$$

or

$$\bar{\psi}_3 = \frac{3\mho^3}{8} \left[4\bar{m}\bar{U}_0(\bar{m} - \bar{U}_0) - \Delta\bar{P} + 2\bar{U}_0\bar{\Sigma} \right] \tag{S70}$$

where we used the expressions for ψ_1 and ψ_3 in eqns (S25) and (S26) as well as the rescaled pressure and tension in eqns (S52) and (S54). It then follows that the Taylor expansion of the rescaled contour curvature

$$\bar{u}(\bar{s}) = R_{\text{ve}} u(s) = R_{\text{ve}} \frac{\mathrm{d}\psi(s)}{\mathrm{d}s} = \frac{1}{\mho} \frac{\mathrm{d}\bar{\psi}(\bar{s})}{\mathrm{d}\bar{s}} \tag{S71}$$

has the form

$$\bar{u}(\bar{s}) = \bar{U}_0 + \frac{1}{2} \frac{\bar{\psi}_3}{\mho} \, \bar{s}^2 + \mathcal{O}(\bar{s}^4) \, . \tag{S72}$$

In addition, the expansion of the rescaled Lagrange multiplier function $\bar{\gamma}$ is given by

$$\bar{\gamma}(\bar{s}) = R_{\text{ve}} \gamma(s) = \bar{\gamma}_1 \bar{s} + \frac{1}{6} \bar{\gamma}_3 \, \bar{s}^3 + \mathcal{O}(\bar{s}^5) \tag{S73}$$

with the coefficients

$$\bar{\gamma}_1 = R_{\text{ve}} s_1 \gamma_1 = \mho \left[2\bar{m}(\bar{m} - \bar{U}_0) + \bar{\Sigma} \right] \tag{S74}$$

and

$$\bar{\gamma}_3 = R_{\text{ve}} s_1^3 \gamma_3 \tag{S75}$$

or

$$\bar{\gamma}_3 = \mho^3 \left[\bar{m}\bar{U}_0(\bar{m} - \bar{U}_0)(\bar{U}_0 - 3\bar{m}) - \frac{1}{4}(9\bar{U}_0 - 3\bar{m})\Delta\bar{P} + \frac{1}{2}\bar{U}_0(\bar{U}_0 - 3\bar{m})\bar{\Sigma} \right] \tag{S76}$$

where eqn (S29) for γ_3 has been used.

Close to the south pole, the rescaled partial area $\Delta\bar{A}$ and the rescaled partial volume $\Delta\bar{V}$ as defined in eqns (S55) and (S57) behave as

$$\Delta\bar{A}(\bar{s}) \approx \frac{\mho^2}{4} \, \bar{s}^2 - \frac{\mho^4}{48} \bar{s}^4 \quad \text{and} \quad \Delta\bar{V}(\bar{s}) \approx \frac{3\mho^4}{16} \bar{s}^4 \tag{S77}$$

for small $\bar{s}$ up to $\mathcal{O}(\bar{s}^4)$.

Regularization of rescaled equations close to north pole. Close to the north pole, we use the dimensionless expansion parameter

$$\bar{\epsilon} \equiv \frac{\epsilon}{s_1} = \frac{s_1 - s}{s_1} = 1 - \bar{s} \quad \text{with} \quad 0 \le \bar{\epsilon} \ll 1, \tag{S78}$$

which measures the arc length from the north pole in units of s_1. We now introduce the functions

$$\bar{r}^{\text{no}}(\bar{\epsilon}) \equiv \bar{r}(\bar{s}) = \frac{r(s)}{R_{\text{ve}}} = \frac{r^{\text{no}}(\epsilon)}{R_{\text{ve}}}\,, \tag{S79}$$

$$\bar{\psi}^{\text{no}}(\bar{\epsilon}) = \pi - \bar{\psi}(\bar{s}) = \pi - \psi(s) = \psi^{\text{no}}(\epsilon)\,, \tag{S80}$$

$$\bar{u}^{\text{no}}(\bar{\epsilon}) \equiv \bar{u}(\bar{s}) = R_{\text{ve}} u(s) = R_{\text{ve}} u^{\text{no}}(\epsilon) \tag{S81}$$

and

$$\bar{\gamma}^{\text{no}}(\bar{\epsilon}) = \bar{\gamma}(\bar{s}) = R_{\text{ve}}\gamma(s) = R_{\text{ve}}\gamma^{\text{no}}(\epsilon) \tag{S82}$$

where the different arc length are related, according to their definitions, via

$$\bar{s} = 1 - \bar{\epsilon}\,, \quad s = s_1\bar{s} = s_1(1-\bar{\epsilon})\,, \quad \text{and} \quad \epsilon = s_1\bar{\epsilon}\,.$$

The expansion of the rescaled radial coordinate $\bar{r}^{\text{no}}$ in powers of $\bar{\epsilon}$ is then given by

$$\bar{r}^{\text{no}}(\bar{\epsilon}) = \bar{r}_1^{\text{no}}\bar{\epsilon} + \frac{1}{6}\bar{r}_3^{\text{no}}\bar{\epsilon}^3 + \mathcal{O}(\bar{\epsilon}^5) \tag{S83}$$

with the coefficients

$$\bar{r}_1^{\text{no}} = \mho r_1^{\text{no}} = \mho \quad \text{and} \quad \bar{r}_3^{\text{no}} = \frac{s_1^3}{R_{\text{ve}}} r_3^{\text{no}} = -\mho^3 \bar{U}_1^2\,. \tag{S84}$$

The expansion of the tilt angle $\bar{\psi}^{\text{no}} = \pi - \bar{\psi}$ has the form

$$\bar{\psi}^{\text{no}}(\bar{\epsilon}) = \bar{\psi}_1^{\text{no}}\bar{\epsilon} + \frac{1}{6}\bar{\psi}_3^{\text{no}}\bar{\epsilon}^3 + \mathcal{O}(\bar{\epsilon}^5) \tag{S85}$$

with the coefficients

$$\bar{\psi}_1^{\text{no}} = \psi_1^{\text{no}} s_1 = U_1 s_1 = \mho \bar{U}_1 \quad \text{and} \quad \bar{\psi}_3^{\text{no}} = \psi_3^{\text{no}} s_1^3 \tag{S86}$$

or

$$\bar{\psi}_3^{\text{no}} = \frac{3\mho^3}{8}\left[4\bar{m}\bar{U}_1(\bar{m} - \bar{U}_1) - \Delta\bar{P} + 2\bar{U}_1\bar{\Sigma}\right] \tag{S87}$$

where eqns (S38) and (S39) for ψ_1^{no} and ψ_3^{no} have been used. It then follows that the rescaled contour curvature

$$\bar{u}^{\text{no}}(\bar{\epsilon}) = R_{\text{ve}} u^{\text{no}}(\epsilon) = R_{\text{ve}} \frac{\mathrm{d}\psi^{\text{no}}(\epsilon)}{\mathrm{d}\epsilon} = \frac{1}{\mho}\frac{\mathrm{d}\psi^{\text{no}}(\bar{\epsilon})}{\mathrm{d}\bar{\epsilon}} \tag{S88}$$

has the expansion

$$\bar{u}^{\text{no}}(\bar{\epsilon}) = \bar{U}_1 + \frac{1}{2}\frac{\bar{\psi}_3^{\text{no}}}{\mho}\,\bar{s}^2 + \mathcal{O}(\bar{\epsilon}^4)\,. \tag{S89}$$

Furthermore, the expansion of the Lagrange multiplier function $\bar{\gamma}^{\text{no}}$ is found to be

$$\bar{\gamma}^{\text{no}}(\bar{\epsilon}) = R_{\text{ve}}\gamma^{\text{no}}(\epsilon) = \bar{\gamma}_1^{\text{no}}\bar{\epsilon} + \frac{1}{6}\bar{\gamma}_3^{\text{no}}\bar{\epsilon}^3 + \mathcal{O}(\bar{\epsilon}^5) \tag{S90}$$

with the coefficients

$$\bar{\gamma}_1^{\text{no}} = R_{\text{ve}}s_1\gamma_1^{\text{no}} = \mho\left[2\bar{m}(\bar{U}_1 - \bar{m}) - \bar{\Sigma}\right] \tag{S91}$$

and

$$\bar{\gamma}_3^{\text{no}} = R_{\text{ve}}s_1^3\gamma_3^{\text{no}} \tag{S92}$$

or

$$\bar{\gamma}_3^{\text{no}} = \mho^3\left[\bar{m}\bar{U}_1(\bar{m} - \bar{U}_1)(3\bar{m} - \bar{U}_1) + \frac{1}{4}(9\bar{U}_1 - 3\bar{m})\Delta\bar{P} + \frac{1}{2}\bar{U}_1(3\bar{m} - \bar{U}_1)\bar{\Sigma}\,.\right] \tag{S93}$$

Close to the north pole, the rescaled partial area behaves as

$$\Delta\bar{A}^{\text{no}}(\bar{\epsilon}) \equiv \frac{\Delta A^{\text{no}}(\epsilon)}{4\pi R_{\text{ve}}^2} = 1 - \frac{1}{4}\mho^2\bar{\epsilon}^2 + \frac{1}{48}\mho^4\bar{U}_1^2\bar{\epsilon}^4 + \mathcal{O}(\bar{\epsilon}^6) \tag{S94}$$

and the rescaled partial volume as

$$\Delta\bar{V}^{\text{no}}(\bar{\epsilon}) \equiv \frac{\Delta V^{\text{no}}(\epsilon)}{\frac{4\pi}{3}R_{\text{ve}}^3} = v - \frac{1}{16}\mho^4\bar{U}_1\bar{\epsilon}^4 + \mathcal{O}(\bar{\epsilon}^6) \tag{S95}$$

where the relationships in eqn (S44) have been used.

S3 Protocol for computation of axisymmetric shapes

To obtain a specific axisymmetric vesicle shape, we solve the rescaled shape equations using the following protocol that consists of four steps.

First, to avoid the numerical instabilities at the south pole with $\bar{s} = 0$, we start from the Taylor expansions close to this pole and choose a certain trial set of the five parameters $\bar{m}$, $\bar{U}_0$, $\Delta\bar{P}$, $\bar{\Sigma}$, and $\mho$ that enter these expansions. We use the Taylor series for $\bar{r}(\bar{s})$ as given by eqn (S66) and calculate the $\bar{r}$-values for $\bar{s} = \bar{s}_n = n\Delta\bar{s}$ with positive integer n and increment $\Delta\bar{s} = 10^{-3}$ until we reach the smallest value $n = n*$ for which $\bar{r}(\bar{s}_{n*}) > 10^{-2}$. The corresponding arc length $\bar{s}_{n*}$ is taken to be the new initial value

$$\bar{s}_{\text{ini}} \equiv \bar{s}_{n*} > 0 \quad \text{of the arc length.} \tag{S96}$$

We then apply the Taylor expansions of all six shape functions $\bar{r}(\bar{s})$, $\bar{\psi}(\bar{s})$, $\bar{u}(\bar{s})$, $\bar{\gamma}(\bar{s})$, $\Delta\bar{A}(\bar{s})$, and $\Delta\bar{V}(\bar{s})$ for small $\bar{s}$ to calculate the values of these functions at the initial arc length $\bar{s} = \bar{s}_{\text{ini}}$. These expansions are provided by eqn (S66) for the radial coordinate $\bar{r}(\bar{s})$, by eqn (S68) for the tilt angle $\bar{\psi}(\bar{s})$, by eqn (S72) for the contour curvature $\bar{u}(\bar{s})$, by eqn (S73) for the Lagrange multiplier function $\bar{\gamma}(\bar{s})$, and by eqn (S77) for the partial membrane area $\Delta\bar{A}(\bar{s})$ and the partial vesicle volume $\Delta\bar{V}(\bar{s})$. In this way, we determine the six initial values $\bar{r}(\bar{s}_{\rm ini})$, $\bar{\psi}(\bar{s}_{\rm ini})$, $\bar{u}(\bar{s}_{\rm ini})$, $\bar{\gamma}(\bar{s}_{\rm ini})$, $\Delta\bar{A}(\bar{s}_{\rm ini})$, and $\Delta\bar{V}(\bar{s}_{\rm ini})$ which are located close to the south pole.

Second, for the given choice of the five parameters $\bar{m}$, $\bar{U}_0$, $\Delta\bar{P}$, $\bar{\Sigma}$, and $\mho$, we start from the six initial values and integrate the six shape eqns (S49), (S50), (S51), (S53), (S56), and (S58) numerically up to the final value

$$\bar{s}_{\rm fin} = 1 - \bar{s}_{\rm ini} \quad \text{of the arc length.} \tag{S97}$$

For this numerical integration, we use the same fixed integration-step $\Delta\bar{s} = 10^{-3}$ and the Julia package DifferentialEquations.jl [3] with the Rodas4 algorithm, corresponding to an implicit Runge-Kutta procedure. As a result of this computation, we obtain the values of the six shape functions at $\bar{s} = \bar{s}_{\rm fin}$ close to the north pole, i.e., the numerical values of $\bar{r}(\bar{s}_{\rm fin})$, $\bar{\psi}(\bar{s}_{\rm fin})$, $\bar{u}(\bar{s}_{\rm fin})$, $\bar{\gamma}(\bar{s}_{\rm fin})$, $\Delta\bar{A}(\bar{s}_{\rm fin})$, and $\Delta\bar{V}(\bar{s}_{\rm fin})$.

Third, we calculate the values of the shape functions at $\bar{s} = \bar{s}_{\rm fin}$ by using the Taylor expansions of these functions in powers of $\bar{\epsilon} = 1 - \bar{s}$, with $\bar{\epsilon} = 0$ at the north pole. The latter expansions are provided by eqn (S83) for the radial coordinate $\bar{r}^{\rm no}(\bar{\epsilon})$, by eqn (S85) for the tilt angle $\bar{\psi}^{\rm no}(\bar{\epsilon})$, by eqn (S89) for the contour curvature $\bar{u}^{\rm no}(\bar{\epsilon})$, by eqn (S90) for the Lagrange multiplier function $\bar{\gamma}^{\rm no}(\bar{\epsilon})$, by eqn (S94) for the partial membrane area $\Delta\bar{A}^{\rm no}(\bar{\epsilon})$, and by eqn (S95) for the partial vesicle volume $\Delta\bar{V}^{\rm no}(\bar{\epsilon})$. These expansions close to the north pole depend on the six parameters $\bar{m}$, $\bar{U}_1$, $\Delta\bar{P}$, $\bar{\Sigma}$, $\mho$, and v.

Finally, we compare the numerical values of the shape functions obtained via the numerical integration for $\bar{s} = \bar{s}_{\rm fin}$ with those obtained from the expansion in powers of $\bar{\epsilon} = 1 - \bar{s}$ for $\bar{\epsilon}_{\rm fin} = 1 - \bar{s}_{\rm fin}$. The six differences as given by $\bar{r}(\bar{s}_{\rm fin}) - \bar{r}^{\rm no}(\bar{\epsilon}_{\rm fin})$ ... $\Delta\bar{V}(\bar{\epsilon}_{\rm fin}) - \Delta\bar{V}^{\rm no}(\bar{\epsilon}_{\rm fin})$ provide the residuals for finding the five parameters $\bar{U}_0$, $\bar{U}_1$, $\Delta\bar{P}$, $\bar{\Sigma}$, and $\mho$ for fixed values of the volume-to-area v and spontaneous curvature $\bar{m}$. The adjustment of the parameters was done with the non-linear trust-region root-finding algorithm provided by the Julia package NLsolve.jl [4].

References

[1] Udo Seifert, Karin Berndl, and Reinhard Lipowsky. Shape transformations of vesicles: Phase diagram for spontaneous- curvature and bilayer-coupling models. *Phys. Rev. A*, 44(2):1182–1202, 1991.

[2] Jaime Agudo-Canalejo and Reinhard Lipowsky. Stabilization of membrane necks by adhesive particles, substrate surfaces, and constriction forces. *Soft Matter*, 12(39):8155–8166, 2016.

[3] Christopher Rackauckas and Qing Nie. DifferentialEquations.jl – A Performant and Feature-Rich Ecosystem for Solving Differential Equations in Julia. *J. Open Res. Softw.*, 2017.

[4] Patrick Kofod Mogensen and Spencer Lyon. JuliaNLSolvers/NLsolve.jl: Zenodo release. may 2019.

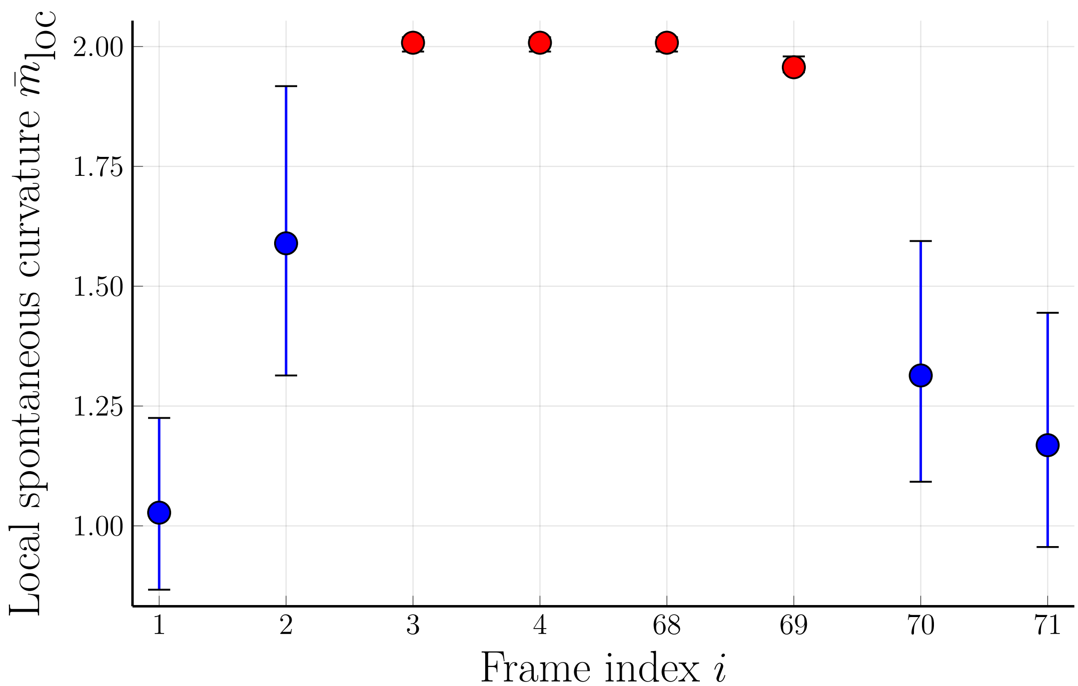

Figure S2: Rescaled local spontaneous curvature $\bar{m}_{\text{loc}}$ versus frame index i. The frame i was taken at time $t = (i-1) \times 7.61\,\text{s}$ after the initial frame with index $i = 1$. The blue data points correspond to up-down symmetric dumbbell shapes, the red data points to asymmetric ones. The symmetry-breaking transformation in Fig. 1 corresponds to $i = 1, 2$, and 3, the symmetry-restoring transformation in Fig. 2 to $i = 68, 69$, and 70. The image $i = 4$ displays a slightly distorted version of $i = 3$ and is thus taken to have the same $\bar{m}_{\text{loc}}$-value as $i = 3$. The image $i = 71$ displays a symmetric dumbbell with an increased neck radius compared to $i = 70$. This increased radius implies the local spontaneous curvature $\bar{m}_{\text{loc}} = 1.17$. The combined sequence of all eight images represents one complete shape oscillation with an average time period of $55.9\,\text{s}$. The error bars are obtained as in Fig. 9.

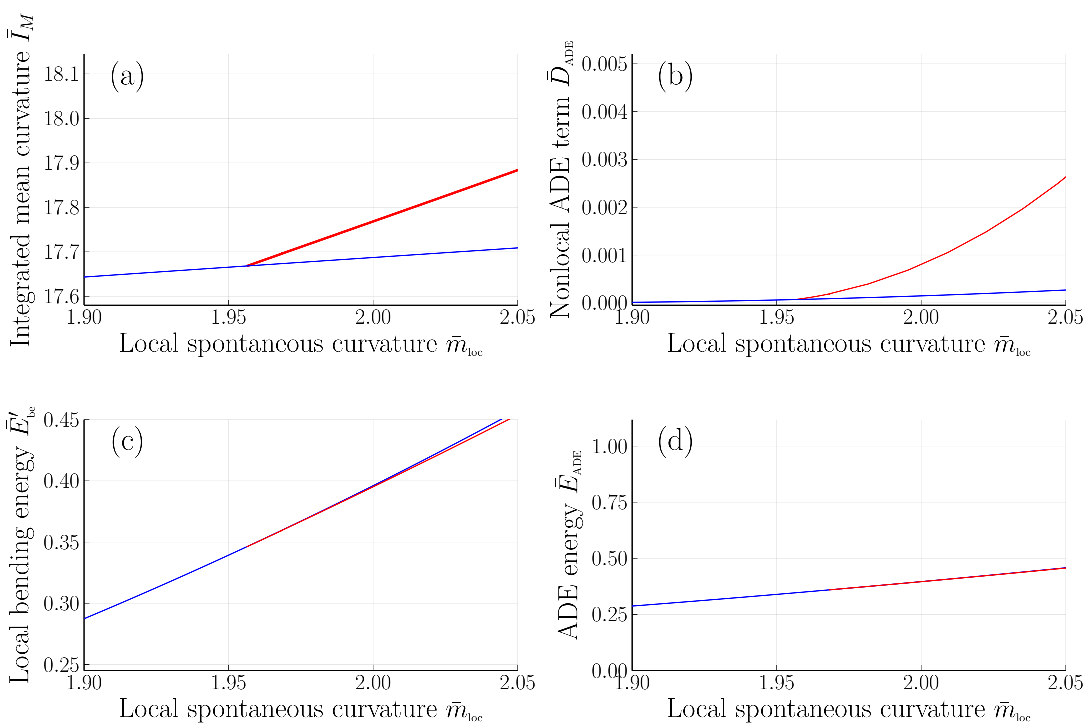

Figure S3: Integrated mean curvature and different energy contributions as functions of the local spontaneous curvature $\bar{m}_{\rm loc}$ for rigidity ratio $\kappa_\Delta/\kappa = 2$. The symmetric and asymmetric branches are displayed as blue and red lines, respectively: (a) Integrated mean curvature $\bar{I}_M$ as in eqn (16); (b) Nonlocal area-difference-elasticity term $\bar{D}_{\rm ADE}$ as in eqn (26); (c) Local bending energy $\bar{E}'_{\rm be}$ as in eqn (25); and (d) ADE energy $\bar{E}_{\rm ADE}$ which is equal to the sum of the local and nonlocal terms in panels b and c. As in Fig. 11, the energy of the asymmetric branch is located below the energy of the symmetric one. All quantities were computed for volume-to-area ratio $v = 0.670$ and reference value $\bar{I}_{M,0} = 17.63$ of the integrated mean curvature.

Movie captions

Movie1. Active shape oscillations of a single GUV: The movie consists of 200 snapshots or frames, each of which displays a different image of the same GUV as obtained by differential interference contrast (DIC) microscopy. The movie was taken with the predefined time interval $\Delta t = 7.61\,\mathrm{s}$ between successive frames and displays the whole series of 200 frames within 20 s, corresponding to about 1500 s or 25 min real time. Apart from a few frames at the beginning and at the end, the movie consists of 26 complete oscillation cycles with an average period of 55.9 s. This movie corresponds to the DIC part of Video_S6 in `https://onlinelibrary.wiley.com/action/downloadSupplement?doi=10.1002%2Fanie.201808750&file=anie201808750-sup-0001-Video_S6.mp4` which is a Supplement to Ref. [4] of the main text.

Movie2. Up-down symmetric and asymmetric dumbbells for fixed volume-to-area ratio $v = 0.670$ and variable spontaneous curvature $\bar{m}$: The left panel displays the up-down symmetric dumbbells (blue) for $0.99 \leq \bar{m} \leq 2.27$, the right panel the up-down asymmetric ones (red), which are present in the restricted $\bar{m}$-range with $1.89 \leq \bar{m} < 1.94$. For $\bar{m} = 1.94$, the branch of asymmetric dumbbells has merged with the branch of symmetric ones. Both types of dumbbells are obtained as smooth solutions of the shape equations for axisymmetric shapes. The rotational symmetry axis is parallel to the z-axis as indicated by the broken vertical lines. The second Cartesian coordinate is taken to be the x-axis.